

UC San Diego

UC San Diego Previously Published Works

Title

Relationship between Ganglion Cell Layer Thickness and Estimated Retinal Ganglion Cell Counts in the Glaucomatous Macula

Permalink

<https://escholarship.org/uc/item/24s8w5xz>

Journal

Ophthalmology, 121(12)

ISSN

0161-6420

Authors

Zhang, Chunwei
Tatham, Andrew J
Weinreb, Robert N
[et al.](#)

Publication Date

2014-12-01

DOI

10.1016/j.opthta.2014.06.047

Peer reviewed

Published in final edited form as:

Ophthalmology. 2014 December ; 121(12): 2371–2379. doi:10.1016/j.ophtha.2014.06.047.

Relationship between Ganglion Cell Layer Thickness and Estimated Retinal Ganglion Cell Counts in the Glaucomatous Macula

Chunwei Zhang, M.D., Ph.D.^{1,2}, Andrew J. Tatham, FRCOphth^{1,3}, Robert N. Weinreb, M.D.¹, Linda M. Zangwill, Ph.D.¹, Zhiyong Yang, M.D., Ph.D.¹, James Z. Zhang, B.S.¹, and Felipe A. Medeiros, M.D., Ph.D.¹

¹Hamilton Glaucoma Center and Department of Ophthalmology, University of California, San Diego

²Department of Ophthalmology, the First Affiliated Hospital, Harbin Medical University, Harbin, China

³Princess Alexandra Eye Pavilion and University of Edinburgh, Edinburgh, United Kingdom

Abstract

Purpose—To investigate the relationship between macular ganglion cell and inner plexiform layer (mGCIPL) thickness and estimated macular retinal ganglion cell (RGC) counts in glaucoma.

Design—Observational cohort study.

Participants—A cross-sectional study of 77 healthy, 154 suspect and 159 glaucomatous eyes from the Diagnostic Innovations in Glaucoma Study (DIGS).

Methods—All eyes had 24-2 Standard Automated Perimetry (SAP) and optic nerve and macular imaging using high definition optical coherence tomography (HDOCT). The total number of RGCs was estimated using a previously described model that utilizes SAP and OCT circumpapillary retinal nerve fiber layer (cpRNFL) measurements. The number of macular RGCs was estimated from the temporal cpRNFL and SAP test points within the central 10 degrees.

Main Outcome Measures—The correlation between mGCIPL thickness and estimates of macular RGC counts.

© 2014 by the American Academy of Ophthalmology. All rights reserved.

Corresponding Author: Felipe A. Medeiros, M.D., Ph.D. Hamilton Glaucoma Center, University of California, San Diego, 9500 Gilman Drive, La Jolla, CA 92093-0946 fmedeiros@ucsd.edu.

Publisher's Disclaimer: This is a PDF file of an unedited manuscript that has been accepted for publication. As a service to our customers we are providing this early version of the manuscript. The manuscript will undergo copyediting, typesetting, and review of the resulting proof before it is published in its final citable form. Please note that during the production process errors may be discovered which could affect the content, and all legal disclaimers that apply to the journal pertain.

The author(s) have made the following disclosure(s):

C.Z. – none; A.J.T. – research support from Heidelberg Engineering; R.N.W. – F: Aerie, Carl Zeiss Meditec, Genentech, Heidelberg Engineering GmbH, National Eye Institute, Nidek, Novartis, Optovue, Topcon; C: Alcon, Allergan, Aquesys, Bausch&Lomb, Topcon; L.M.Z – F: Carl-Zeiss Meditec, Heidelberg Engineering, Topcon and Nidek; J. Z. – none; Z. Y. – none; A.M. – F: Alcon Laboratories, Bausch & Lomb, Carl Zeiss Meditec, Heidelberg Engineering, Merck, Allergan, Sensimed, Topcon, Reichert, National Eye Institute, R: Alcon Laboratories, Allergan, Carl Zeiss Meditec, Reichert, C: Allergan, Carl-Zeiss Meditec, Novartis.

Results—The average estimated macular RGC count in glaucomatous eyes was $306,010 \pm 109,449$ cells, which was significantly lower than the estimate of $520,678 \pm 106,843$ cells in healthy eyes ($P < 0.001$). Glaucomatous eyes had 41% fewer estimated macular RGCs than healthy eyes and suspects 21% fewer. There was strong correlation between estimated macular RGC counts and mGCIPL thickness ($R^2 = 0.67$; $P < 0.001$). Macular RGC counts performed better than average mGCIPL thickness in discriminating healthy and glaucomatous eyes with receiver operating characteristic (ROC) curve areas of 0.873 and 0.775, respectively ($P = 0.015$).

Conclusions—The strong association between estimated macular RGC counts and mGCIPL thickness and the better diagnostic performance of the macular RGC counts compared to mGCIPL thickness provides further evidence that estimates of RGC number from cpRNFL thickness and SAP sensitivity can be used to assess neural losses in glaucoma.

Glaucoma is characterized by dysfunction and loss of retinal ganglion cells (RGCs), with resultant structural changes to the optic nerve head, retinal nerve fiber layer (RNFL) and ganglion cell-inner plexiform layer, and loss of visual field.⁽¹⁾ The goal of glaucoma management is to slow down the rate of progressive neural losses and to preserve visual function. As the macula has the highest density of RGCs,^(2,3) macular imaging may be a valuable method of assessing neural damage in glaucoma. In fact, approximately 50% of RGCs are located within 4.5 mm (16-degrees) of the foveal center, a region that comprises only 7.3% of the total retinal area.⁽⁴⁾ Furthermore, the macula is vital for central vision and therefore loss of macular RGCs is likely to be of particular importance for vision-related quality of life. Although it has long been recognized that glaucomatous damage also affects the macula, evaluation of structural changes in glaucoma has primarily focused on the optic disc and circumpapillary region.^(5–8) Using optical coherence tomography (OCT) it is now possible to obtain objective measurements of macular structures, including the ganglion cell layer, which is the location of ganglion cell bodies.⁽⁹⁾

Loss of retinal thickness can be used as a surrogate for loss of RGC axons and cell bodies.^(8,10–15) Devices such as Cirrus HDOCT provide a means to quantify thickness of individual retinal layers. Recent studies have shown that the macular ganglion cell complex (mGCC) thickness, which includes the macular RNFL, ganglion cell layer and inner plexiform layer has good diagnostic accuracy for glaucoma.^(16–18) The Cirrus HDOCT also includes a ganglion cell analysis algorithm that is able to detect and measure the thickness of the macular ganglion cell inner plexiform layer (mGCIPL) with excellent reproducibility.^(19,20) However, unlike the mGCC, the mGCIPL analysis does not include the RNFL and, therefore, is more likely to reflect the actual number of RGC bodies. Mwanza and colleagues recently reported that mGCIPL measurements had similar ability to detect glaucoma compared to circumpapillary RNFL thickness measurements (cpRNFL).⁽²⁰⁾

Even though mGCIPL measurements may better reflect RGC counts, no study has yet evaluated the relationship between this parameter and the number of macular RGCs in vivo. Although the direct quantification of RGCs is not yet possible in vivo, empirical formulas derived from experimental studies in non-human primates, and validated in human cohorts, may be used to estimate the number of RGCs from cpRNFL thickness measurements and standard automated perimetry (SAP) sensitivities.^(21–24) Medeiros and colleagues proposed

a method of combining RGC estimates from structural and functional measures and the combined RGC estimates have been shown to perform significantly better than isolated structural and functional parameters for staging glaucoma and monitoring progression.^(23,25,26)

The purpose of this study was to evaluate the relationship between OCT-derived measurements of macular thickness, specifically the mGCIPL, and the estimated number of macular RGCs in healthy, suspect and glaucomatous eyes. We also compared the ability of mGCIPL thickness and estimated number of RGCs to differentiate healthy and glaucomatous eyes.

METHODS

This was a cross-sectional observational study of participants from the Diagnostic Innovations in Glaucoma Study (DIGS) at the University of California San Diego (UCSD). The DIGS is a prospective longitudinal study designed to evaluate optic nerve structure and visual function in glaucoma. All participants provided written informed consent, and the institutional review board and human subjects committee at UCSD prospectively approved all methods. All study methods adhered to the tenets of the Declaration of Helsinki for research involving human subjects and the study was conducted in accordance with the regulations of the Health Insurance Portability and Accountability Act. Methodological details have previously been described in detail.⁽²⁷⁾

At each visit subjects underwent a comprehensive ophthalmologic examination including review of medical history, best-corrected visual acuity, slit-lamp biomicroscopy, measurement of intraocular pressure (IOP), dilated fundoscopic examination, stereoscopic optic disc photography, and automated perimetry using the Swedish interactive threshold algorithm (SITA Standard testing algorithm 24-2). Subjects were excluded if they presented with a best-corrected visual acuity < 20/40, spherical refraction outside ± 5.0 diopters, and/or cylinder correction outside 3.0 diopters, or any other ocular or systemic disease that could affect the optic nerve or the visual field. Only subjects with open angles on gonioscopy were included.

The study included 390 eyes of 224 participants. There were 77 healthy eyes, 154 eyes with suspected glaucoma and 159 eyes with glaucoma. Glaucoma was diagnosed based on the presence of repeatable (3 consecutive) abnormal SAP test results on the 24-2 program of the visual field (Humphrey Field Analyzer [HFA II-i]; Carl Zeiss Meditec, Inc., Dublin, CA) or if progressive glaucomatous optic disc changes were noted on masked examination of stereophotographs, regardless of the results of SAP. Optic disc stereophotographs were graded at UCSD Optic Disc Reading Center, details of which have been provided elsewhere.⁽²⁷⁻²⁹⁾ For the purposes of this study we defined an abnormal SAP result as one with a pattern standard deviation (PSD) outside the 95% confidence limits or a glaucoma hemifield test result outside the reference range. Eyes were deemed to have suspect glaucoma if the optic disc appearance was suspicious of glaucoma on masked stereophotograph assessment but there was no repeatable SAP abnormality. A suspicious optic disc appearance was defined by the presence of neuroretinal rim thinning or RNFL

defects. Glaucoma suspects also included eyes with IOP > 21 mm Hg, but with healthy appearing optic discs and without repeatable abnormal SAP results. Healthy subjects were recruited from the general population through advertisements and from the staff and employees of the University of California, San Diego. Healthy eyes were recruited from the general population and had IOP \leq 21 mmHg, with no history of increased IOP.

Optical Coherence Tomography

The Cirrus HDOCT (software version 6.5; Carl Zeiss Meditec, Inc. Dublin, CA) was used to acquire cpRNFL and mGCIPL measurements. This device has been described in detail previously.⁽²⁶⁾ cpRNFL thickness measurements were acquired using the optic disc cube 200 \times 200 protocol. This protocol utilizes a 3-dimensional (3D) scan of a 6 \times 6 mm area centered on the optic disc. Average cpRNFL thickness is then automatically calculated from a 3.46-mm diameter circular scan (10,870 μ m in length) placed around the optic disc. The macular cube 200 \times 200 protocol was used to acquire macular thickness data. This protocol is based on a 3-dimensional scan centered on the macula in which information from a 1024 (depth) \times 200 \times 200 point parallelepiped is collected. The ganglion cell analysis algorithm automatically segmented the GCIPL based on three-dimensional data generated from the macular cube scan protocol. The algorithm automatically segmented the outer boundary of RNFL and the outer boundary of IPL at the macular region; this segmented layer yielded GCIPL thickness. A detailed description of the algorithm has been previously presented.^(19,30) The Cirrus HDOCT images were reviewed and included if the signal strength was >7, if movement artifacts and segmentation errors were absent, and there was good centering on the optic disc or fovea for the optic disc and macular cube protocols, respectively.

Standard Automated Perimetry

All patients underwent SAP testing using the SITA Standard 24-2 strategy within 6 months of HDOCT. All visual fields evaluated by the UCSD Visual Field Assessment Center (VisFACT).⁽³¹⁾ Fields with more than 33% fixation losses or false-negative errors, or more than 15% false-positive errors, were excluded. The only exception was the inclusion of tests with false-negative errors of more than 33% in the presence of advanced disease. Visual fields exhibiting a learning effect were also excluded. A learning effect was defined as initial tests showing consistent improvement on visual field indices. Visual fields were further reviewed for artifacts including eyelid and rim artifacts, fatigue effects, inappropriate fixation, and evidence that the visual field results were caused by a disease other than glaucoma and inattention. The UCSD Visual Field Assessment Center requested repeats of unreliable visual field test results, and these were obtained whenever possible.

Estimation of Macular Retinal Ganglion Cell Number

Numbers of retinal ganglion cells were estimated using the model described by Medeiros and colleagues^(22–24) which is based on empirical formulas developed by Harwerth and colleagues⁽²¹⁾ for estimating RGC counts from SAP and OCT. The formulas were derived from experimental research in monkeys and subsequently translated to human eyes. Using these formulas it is possible to use information from both structural and functional tests to derive a final combined estimate of the RGC count in a particular eye. The details of the

model and the empirical formulas used to derive RGC counts have been described in detail previously.⁽²²⁻²⁴⁾ In brief, the number of RGC somas in an area of the retina corresponding to a specific SAP test field location at eccentricity ec with sensitivity s in dB was estimated using the formulas below, where m and b represent the slope and intercept respectively of the linear function relating ganglion cell quantity (gc) in dB to the visual field sensitivity (s) in dB at a given eccentricity.:

$$m = [0.054*(ec*1.32)] + 0.9$$

$$b = [-1.5*(ec*1.32)] - 14.8$$

$$gc = \{[(s-1)-b]/m\} + 4.7$$

$$SAPrgc = \Sigma 10^{(gc*0.1)}$$

The SAP-derived estimate of the total number of RGCs ($SAPrgc$) was calculated by considering the cell density derived from each perimetry measurement to be uniform over an area of retina corresponding to the 6×6 degree area of visual space that separates test locations in SAP. $SAPrgc$ incorporated information from each test location of the 24-2 visual field. However, for the purposes of the present study we were also interested in estimating macula RGC counts. To estimate the number of RGCs located in the macula from SAP (macular $SAPrgc$) we summed the RGC estimates from the central 16 points of the 24-2 SAP test, test locations representing the central 10-degrees (Figure 1A).

The structural part of the model consisted of estimating the number of RGC axons from cpRNFL thickness measurements obtained by OCT. The model took into account the effect of aging on axonal density and the effect of disease severity on the relationship between neuronal and non-neuronal components of the RNFL. The method of estimating total RGC counts from OCT has been described previously.⁽²²⁻²⁴⁾ To obtain an estimate of the number of macular RGCs (macular $OCTrgc$), we calculated the average cpRNFL thickness in the temporal, superotemporal and inferotemporal regions that likely correspond to region of RGC axons emanating from RGCs in the macular region (Figure 1B).⁽⁹⁾ The following formulas were applied:

$$d = (-0.007*age) + 1.4$$

$$c = (-0.26*macular TD) + 0.12$$

$$a = \text{average temporal cpRNFL thickness} * 0.5 * 10870 * d$$

$$\text{Macular } OCTrgc = 10^{[(\log(a)*10 - c)*0.1]}$$

In the above formulas, d corresponds to the axonal density (axons/ μm^2) and c is a correction factor for the severity of disease to take into account remodeling of the RNFL axonal and non-axonal composition. Macular total deviation (TD) is the average TD in decibels of the 24-2 SAP test points corresponding to the central 10 degrees.

In summary, the above formulas provide a means to estimate of the number of total and macular RGCs from two sources, one functional and one structural. A combined estimation of total RGC counts was performed according to the following formula previously described by Medeiros and colleagues⁽²²⁻²⁴⁾:

$$\text{Estimated total RGC count} = (1 + \text{MD}/30) * \text{OCT}_{\text{rgc}} + (-\text{MD}/30) * \text{SAP}_{\text{rgc}}$$

Estimated macular RGC counts were similarly calculated using macular OCT_{rgc} , macular SAP_{rgc} estimates and macular TD. The rationale for using a weighting system for deriving the final RGC count has been described previously but in essence it relies on the fact that the accuracies of clinical perimetry and imaging tests are inversely related to disease severity.^(22–24)

Statistical Analysis

Normality assumption was assessed by inspection of histograms and using Shapiro–Wilk tests. Student t-tests were used for group comparison for normally distributed variables and Wilcoxon rank-sum test for continuous non-normal variables. The relationship between estimated macular RGC counts and average mGCIPL thickness was initially examined using scatterplots. Linear regression was then used to examine the relationship between estimated macular RGC counts and average mGCIPL thickness. As observations from two eyes of the same subject are likely to be correlated, a between-cluster variance estimator was used in the regression analysis to account for correlations between eyes of the same subject and calculate robust variance estimates.⁽³²⁾

To evaluate the ability of the parameters to differentiate between controls and glaucomatous eyes, area under the ROC curves (AUC) was used to summarize diagnostic accuracy. A ROC curve is a plot of the true-positive rate versus the false-positive rate for all possible cut-points. A ROC curve area of 1 represents perfect discrimination, whereas an area of 0.5 represents chance discrimination. The ROC curve areas and 95% confidence intervals were obtained for each parameter after adjusting for age, using a previously described method.^(33,34) All statistical analyses were performed with commercially available software (STATA, version 13; Stata Corp LP, College Station, TX). The alpha level (type I error) was set at 0.05.

RESULTS

The mean (\pm standard deviation) age of participants was 64.7 ± 15.6 years, however, the healthy participants were significantly younger than those with glaucoma and suspected glaucoma ($P < 0.001$ for both comparisons). 145 of 224 subjects (64.7%) were of European descent and 63 of 224 subjects (28.1%) were of African descent. 117 of 224 subjects (52.2%) were female. The demographic and clinical characteristics, including the results of estimation of total RGC and macular RGC number are summarized in Table 1. Eyes with glaucoma had significantly worse SAP mean deviation (MD) and thinner cpRNFL than healthy eyes ($P < 0.001$ for both comparisons). Of the 159 glaucomatous eyes, 139 (87.4%) had repeatable (≥ 3 consecutive) abnormal SAP tests. The average SAP MD in glaucomatous eyes was -5.06 ± 5.43 dB. The average cpRNFL thickness was 95.03 ± 13.10 μm , 85.74 ± 13.38 μm and 71.92 ± 18.28 μm in healthy, suspect glaucoma and glaucoma, respectively ($P < 0.001$). Eyes with glaucoma also had and significantly worse macular SAP TD (i.e., TD of the 16 macular SAP test locations) than healthy eyes (-0.51 dB versus -2.91 dB respectively, $P < 0.001$). Average mGCIPL thicknesses were 81.40 ± 6.71 μm , $75.55 \pm$

7.17 μm and $67.98 \pm 10.73\mu\text{m}$ in healthy, suspect glaucoma and glaucoma, respectively ($P < 0.001$).

The average estimated number of macular RGCs in glaucomatous eyes was $306,010 \pm 109,447$ cells, which was significantly lower than the estimated count of $410,003 \pm 83,887$ cells in eyes with suspect glaucoma and $520,678 \pm 106,843$ cells in healthy eyes ($P < 0.001$). The average total estimated number of RGCs was $1,042,019 \pm 185,243$ in healthy eyes, $812,458 \pm 163,151$ in eyes with suspect glaucoma and $570,433 \pm 207,525$ in eyes with glaucoma (Table 1). Therefore in the estimated macular RGC count represented approximately 50% of the total estimated number of RGCs. Figure 2 shows the distribution of macular RGC and total RGC estimates in healthy, suspected glaucoma and glaucomatous eyes. Compared to the estimated number of macular RGCs in healthy eyes, eyes with glaucoma had on average 41% fewer macular RGCs and eyes with suspected glaucoma had on average 21% fewer macular RGCs. Glaucomatous eyes had 45% fewer estimated total RGCs than healthy eyes and suspects 22% fewer.

Average mGCIPL thickness measurements were strongly correlated with the estimated number of macular RGCs ($R^2 = 0.67$; $P < 0.001$) (Figure 3A). There was also strong correlation between mGCIPL thickness measurements and the estimated total number of RGCs ($R^2 = 0.63$; $P < 0.001$) (Figure 3B).

The macular RGC counts performed significantly better than the HDOCT average mGCIPL thickness parameter in discriminating glaucomatous from healthy eyes with age-adjusted ROC curve areas of 0.873 (95% CI 0.809 – 0.922) versus 0.775 (95% CI 0.675 – 0.858), respectively ($P = 0.015$) (Figure 4). For 95% specificity, macular RGC counts had a sensitivity of 72%. At the same specificity, HDOCT average mGCIPL thickness had a sensitivity of 54%. For 90% specificity, sensitivity of macular RGC counts increased to 76% versus 60% for HDOCT average mGCIPL thickness. Total estimated RGC count had an AUC of 0.932 (95% CI 0.885 – 0.963). The AUCs of average cpRNFL thickness and SAP MD (i.e., including all 24-2 test locations) were 0.856 (95% CI 0.778 – 0.913) and 0.610 (95% CI 0.183 – 0.812), respectively.

Examples of two eyes included in the study, including the estimates of macular RGC count, estimates of total RGC count and average mGCIPL thicknesses are shown in Figures 5 and Figures 6.

DISCUSSION

OCT measurements of the thickness of the ganglion cell layer currently represent the best imaging estimate of the quantity of RGCs in the macular area. In the present study, we found a strong relationship between estimates of macular RGC counts and the OCT parameter mGCIPL ($R^2 = 67\%$), which gives further support to the validity of the method used for estimating RGC counts. In addition, we showed that estimates of RGC counts actually performed better than isolated OCT macular measurements for diagnosing glaucoma, a result that may have significant implications for using these methods in detecting glaucomatous damage in clinical practice.

Although strong, the correlation between estimated RGC counts and mGCIPL was not perfect. This finding may have several explanations, such as measurement variability, variability among individuals in the position of the disc relative to the macula, and the fact that mGCIPL incorporates not only the thickness of the ganglion cell layer, but also that of the inner plexiform layer. Therefore, changes to the inner plexiform layer could influence mGCIPL thickness without translating into losses of RGCs. In addition, it is known that amacrine cells permeate the ganglion cell layer and, therefore, contribute to its thickness^(35–37) in a way that is not directly relate to RGC counts.

In our study, healthy eyes had an average estimated total of 520,678 RGCs in the macular region, corresponding to approximately 50% of the total estimated count of 1,042,019 cells. This number is similar to those found in previous histological studies. For example, Curcio and colleagues reported that approximately 50% of RGCs are located within the macula, with RGC densities reaching 32,000–38,000 cells/mm² up to 2.0 mm from the center of the fovea.⁽⁴⁾ Eyes with suspected glaucoma had significantly lower estimated RGC counts than healthy eyes for macular and total estimates. The average estimated RGC count in glaucoma suspects was 812,458 cells, with 410,003 RGC in the macular region, representing a reduction in estimated RGC count of 22.0% and 21.3% for total and macular regions respectively compared to healthy eyes. Eyes with glaucoma had even lower estimated numbers of RGCs. The average estimated macular RGC count in glaucoma was 306,010 cells which was approximately 41% lower than the estimated number found in healthy eyes. Interestingly, the estimated proportion of RGCs lost in the macula in glaucomatous compared to healthy eyes was similar to the estimated proportion of total RGCs lost (41% versus 45% fewer RGCs compared to healthy eyes for macular and total RGC estimates, respectively). This seems to indicate that glaucomatous damage affects both macular and extra-macular regions to a similar degree. Although eyes with glaucoma had large estimated macular RGC losses, the average loss of SAP sensitivity in this region was only –2.9 dB. This observation seems to be in agreement with previous studies indicating that large numbers of RGCs may need to be lost before statistically significant abnormalities are detectable on SAP.^(21,26,38) This is likely to be particularly relevant in the macula where the density of RGCs is high.

The combined structure-function estimate of macular RGC numbers had better ability to distinguish healthy and glaucomatous eyes than isolated mGCIPL thickness with age-adjusted AUCs of 0.873 and 0.775, respectively ($P = 0.015$). However, despite the good diagnostic ability of macular RGC counts, the best performing parameter for discriminating glaucomatous from healthy eyes was the total estimated number of RGCs, which had an AUC of 0.932. The lower diagnostic ability of macular parameters is to be expected as macular analysis is based on sampling of only 50% of the RGC population. In contrast, cpRNFL measurements include axons from the entire retina and therefore could detect glaucomatous changes in non-macular locations.

Although not all RGCs are located in the macula, it is an attractive region for imaging in glaucoma due to its importance for central vision and its relative consistent structure between individuals.⁽¹⁹⁾ Macular measurements may be less affected by non-neural structures such as blood vessels than the cpRNFL and, therefore, less prone to segmentation

software failures during OCT imaging. The macula may also be affected in early glaucoma, and some previous studies have indicated macular thickness measurements to have similar ability as cpRNFL to detect glaucoma.^(20,39) A recent study, however, has shown that when macular ganglion cell complex thickness is used to detect preperimetric glaucoma it performs less well than cpRNFL thickness.⁽⁴⁰⁾ Lisboa and colleagues reported AUCs of 0.79 and 0.89 for macular ganglion cell complex and cpRNFL average thickness values, respectively.⁽⁴⁰⁾ It is also possible that differences in the location of glaucomatous damage may have led to differences in results, with macular measurements likely to be a good diagnostic marker in eyes with macular damage, while performing less well in eyes with only extra-macular damage. Nevertheless, our study indicates that by combining structural and functional information using the common metric of RGC counts it is possible to provide a more sensitive marker for the presence of macular damage. It is possible, however, that the incorporation of functional information derived from visual fields using 10-2 pattern of stimuli could potentially improve the characterization of macular damage, as this test evaluates a much larger number of points in the macular area compared to the 24-2 test. Future studies should investigate whether the use of 10-2 fields combined with structural info improves on the detection of macular damage obtained with the methods presented in this study.

The relationship between SAP sensitivity and mGCIPL thickness (and underlying numbers of RGCs) may be affected by changes in spatial summation.⁽⁴¹⁻⁴³⁾ If the area of a perimetric test stimulus is smaller than a critical area (Ricco's area), the sensitivity threshold is determined by complete spatial summation. In contrast, if the stimulus is larger than Ricco's area, probability summation occurs.⁽⁴¹⁾ Ricco's area enlarges with increasing eccentricity and in the healthy eye, using the Goldmann size III stimulus, spatial summation is complete only at retinal eccentricities of greater than approximately 15 degrees. Therefore in the healthy macula spatial summation is incomplete with the result that the relationship between RGC density and SAP sensitivity thresholds is shallower in the macula than in more peripheral regions.^(41,43) Further studies are need to examine the effect of changes in the area of spatial summation on the relationship between SAP sensitivity and mGCIPL thickness, particularly as in glaucoma loss of RGCs may cause enlargement of the area of complete summation.⁽⁴¹⁾

This present study has limitations. We used empirically derived formulas to estimate the number of macular RGCs. Although these estimates have been validated in histologic studies in monkeys and also have been applied to multiple external cohorts in humans,⁽²¹⁾ such validation was not based on direct histologic RGC counts in humans. However, this limitation applies to most measurements obtained in clinical practice from imaging devices and other instruments and the formulas have been validated in multiple external human cohorts.^(22-24,44) A further limitation is that although the temporal cpRNFL thickness was used for the structural component of the macular RGC estimate, the exact location of the axons from macular RGCs is not known and may vary between individuals. Furthermore, although the ONH and macular scans were acquired sequentially, and scans were reviewed by the imaging center, there may have been small undetected differences in patient head or eye position that could have influenced measurements. Future improvements in scan acquisition and processing technology such as Fovea-Bruch's Membrane Opening (fovea-

BMO) alignment may help improve the correlation between cpRNFL and mGCIPL measurements.⁽⁴⁵⁾ Another limitation of our study is related to the difficulty in applying a proper reference standard when evaluating the diagnostic accuracy of a combined structure and function method. We attempted to overcome this limitation by including as glaucomatous eyes those that had visual field defects, as well as those with evidence of progressive optic disc damage on photographs, regardless of field results. Such classification represents currently acceptable clinical standards in the diagnosis of glaucoma, which the combined metric wants to mimic. Healthy eyes were selected from the general population, without history of elevated IOP, but visual fields or optic nerve assessment were not used for classification, in order to avoid potential bias.

Although in the present study, patients with suspected glaucoma and glaucoma were older than healthy subjects, this is unlikely to have had a significant impact on the study conclusions. Previous studies have shown that RGC loss occurs with normal aging, however, the estimated rate is relatively slow and therefore would not account for the large differences in RGC estimates between groups.^(24, 38) Furthermore differences in age between groups were corrected for in the ROC regression models examining diagnostic ability of each parameter.

In conclusion, this study demonstrates a strong relationship between mGCIPL thickness and estimates of macular RGC count, which provides further evidence that estimates of RGC count can be used to assess neural losses in glaucoma. Moreover the accuracy of estimates of neuronal loss was enhanced by combining information from structural and functional domains, with stronger correlation between RGC estimates and mGCIPL thickness than between isolated measures of structure and function and mGCIPL thickness.

Acknowledgments

Supported in part by National Institutes of Health/National Eye Institute grants EY021818 F.A.M.), EY11008 (L.M.Z.), EY14267 (L.M.Z.), EY019869 (L.M.Z.), core grant P30EY022589; an unrestricted grant from Research to Prevent Blindness (New York, NY); grants for participants' glaucoma medications from Alcon, Allergan, Pfizer, Merck and Santen; Natural Science Foundation of Heilongjiang Province for Returned Scholars, China. No.LC2012C21; Innovation research special fund of the Science and Technology of Harbin of Heilong Jiang Province, China. No.2011RFLYS029. Scientific and technical research fund of Education Bureau of Heilongjiang Province, China. No.12511311.

References

1. Weinreb RN, Aung T, Medeiros FA. The pathophysiology and treatment of glaucoma: a review. *JAMA*. 2014; 311:1901–1911. [PubMed: 24825645]
2. Knighton RW, Gregori G. The shape of the ganglion cell plus inner plexiform layers of the normal human macula. *Invest Ophthalmol Vis Sci*. 2012; 53:7412–7420. [PubMed: 23033389]
3. Hood DC, Raza AS, de Moraes CG, et al. Initial arcuate defects within the central 10 degrees in glaucoma. *Invest Ophthalmol Vis Sci*. 2011; 52:940–946. [PubMed: 20881293]
4. Curcio CA, Allen KA. Topography of ganglion cells in human retina. *Journal of Comparative Neurology*. 1990; 300:5–25. [PubMed: 2229487]
5. Aulhorn E, Karmeyer H. Frequency distribution in early glaucomatous visual field defects. *Doc Ophthalmol Proc Ser*. 1977; 14:75–83.
6. Anctil JL, Anderson DR. Early foveal involvement and generalized depression of the visual field in glaucoma. *Arch Ophthalmol*. 1984; 102:363–370. [PubMed: 6703983]

7. Nicholas SP, Werner EB. Location of early glaucomatous visual field defects. *Can J Ophthalmol*. 1980; 15:131. [PubMed: 7437940]
8. Zeimer R, Asrani S, Zou S, Quigley H, et al. Quantitative detection of glaucomatous damage at the posterior pole by retinal thickness mapping. A pilot study. *Ophthalmology*. 1998; 105:224–231. [PubMed: 9479279]
9. Hood DC, Raza AS, de Moraes CG, et al. Glaucomatous damage of the macula. *Prog Retin Eye Res*. 2013; 32:1–21. [PubMed: 22995953]
10. Medeiros FA, Zangwill LM, Bowd C, et al. Evaluation of retinal nerve fiber layer, optic nerve head, and macular thickness measurements for glaucoma detection using optical coherence tomography. *Am J Ophthalmol*. 2005; 139:44–55. [PubMed: 15652827]
11. Tan O, Chopra V, Lu AT-H, et al. Detection of macular ganglion cell loss in glaucoma by fourier-domain optical coherence tomography. *Ophthalmology*. 2009; 116:2305–2314. [PubMed: 19744726]
12. Kotera Y, Hangai M, Hirose F, et al. Three-dimensional imaging of macular inner structures in glaucoma by using spectral-domain optical coherence tomography. *Invest Ophthalmol Vis Sci*. 2011; 52:1412–1421. [PubMed: 21087959]
13. Nakatani Y, Higashide T, Ohkubo S, et al. Evaluation of macular thickness and peripapillary retinal nerve fiber layer thickness for detection of early glaucoma using spectral domain optical coherence tomography. *J Glaucoma*. 2011; 20:252–259. [PubMed: 20520570]
14. Rao HL, Zangwill LM, Weinreb RN, et al. Comparison of different spectral domain optical coherence tomography scanning areas for glaucoma diagnosis. *Ophthalmology*. 2010; 117:1692–1699. [PubMed: 20493529]
15. Seong M, Sung KR, Choi EH, et al. Macular and peripapillary retinal nerve fiber layer measurements by spectral domain optical coherence tomography in normal-tension glaucoma. *Invest Ophthalmol Vis Sci*. 2010; 51:1446–1452. [PubMed: 19834029]
16. Garas A, Vargha P, Holló G. Diagnostic accuracy of nerve fibre layer, macular thickness and optic disc measurements made with the rtvue-100 optical coherence tomograph to detect glaucoma. *Eye (Lond)*. 2011; 25:57–65. [PubMed: 20930859]
17. Kim NR, Lee ES, Seong GJ, et al. Comparing the ganglion cell complex and retinal nerve fibre layer measurements by fourier domain OCT to detect glaucoma in high myopia. *Br J Ophthalmol*. 2011; 95:1115–1121. [PubMed: 20805125]
18. Tan O, Chopra V, Lu AT, et al. Detection of macular ganglion cell loss in glaucoma by fourier-domain optical coherence tomography. *Ophthalmology*. 2009; 116:2305–2314. [PubMed: 19744726]
19. Mwanza JC, Oakley JD, Budenz DL, et al. Macular ganglion cell-inner plexiform layer: Automated detection and thickness reproducibility with spectral domain-optical coherence tomography in glaucoma. *Invest Ophthalmol Vis Sci*. 2011; 52:8323–8329. [PubMed: 21917932]
20. Mwanza JC, Durbin MK, Budenz DL, et al. Glaucoma diagnostic accuracy of ganglion cell-inner plexiform layer thickness: Comparison with nerve fiber layer and optic nerve head. *Ophthalmology*. 2012; 119:1151–1158. [PubMed: 22365056]
21. Harwerth RS, Wheat JL, Fredette MJ, et al. Linking structure and function in glaucoma. *Prog Retin Eye Res*. 2010; 29:249–271. [PubMed: 20226873]
22. Medeiros FA, Lisboa R, Weinreb RN, et al. A combined index of structure and function for staging glaucomatous damage. *Arch Ophthalmol*. 2012; 130:1107–1116. [PubMed: 23130365]
23. Medeiros FA, Zangwill LM, Bowd C, et al. The structure and function relationship in glaucoma: Implications for detection of progression and measurement of rates of change. *Invest Ophthalmol Vis Sci*. 2012; 53:6939–6946. [PubMed: 22893677]
24. Medeiros FA, Zangwill LM, Anderson DR, et al. Estimating the rate of retinal ganglion cell loss in glaucoma. *Am J Ophthalmol*. 2012; 154:814.e1–824.e1. [PubMed: 22840484]
25. Marvasti AH, Tatham AJ, Zangwill LM, et al. The relationship between visual field index and estimated number of retinal ganglion cells in glaucoma. *PLoS One*. 2013; 8:e76590. [PubMed: 24146895]

26. Medeiros FA, Lisboa R, Weinreb RN, et al. Retinal ganglion cell count estimates associated with early development of visual field defects in glaucoma. *Ophthalmology*. 2013; 120:736–744. [PubMed: 23246120]
27. Sample PA, Girkin CA, Zangwill LM, et al. The african descent and glaucoma evaluation study (ADAGES): Design and baseline data. *Arch Ophthalmol*. 2009; 127:1136–1145. [PubMed: 19752422]
28. Medeiros FA, Weinreb RN, Sample PA, et al. Validation of a predictive model to estimate the risk of conversion from ocular hypertension to glaucoma. *Arch Ophthalmol*. 2005; 123:1351–1360. [PubMed: 16219726]
29. Medeiros FA, Vizzeri G, Zangwill LM, et al. Comparison of retinal nerve fiber layer and optic disc imaging for diagnosing glaucoma in patients suspected of having the disease. *Ophthalmology*. 2008; 115:1340–1346. [PubMed: 18207246]
30. Tham YC, Cheung CY, Koh VT, et al. Relationship between ganglion cell-inner plexiform layer and optic disc/retinal nerve fibre layer parameters in non-glaucomatous eyes. *Br J Ophthalmol*. 2013; 97:1592–1597. [PubMed: 24123901]
31. Racette L, Liebmann JM, Girkin CA, et al. African descent and glaucoma evaluation study (ADAGES): III. Ancestry differences in visual function in healthy eyes. *Arch Ophthalmol*. 2010; 128:551–559. [PubMed: 20457975]
32. Williams RL. A note on robust variance estimation for cluster-correlated data. *Biometrics*. 2000; 56:645–646. [PubMed: 10877330]
33. Alonzo TA, Pepe MS. Distribution-free ROC analysis using binary regression techniques. *Biostatistics*. 2002; 3:421–432. [PubMed: 12933607]
34. Medeiros FA, Sample PA, Zangwill LM, et al. A statistical approach to the evaluation of covariate effects on the receiver operating characteristic curves of diagnostic tests in glaucoma. *Invest Ophthalmol Vis Sci*. 2006; 47:2520–2527. [PubMed: 16723465]
35. Mitrofanis J, Provis JM. A distinctive soma size gradient among catecholaminergic neurones of human retinae. *Brain Res*. 1990; 527:69–75. 10. [PubMed: 1980840]
36. Kolb H, Linberg KA, Fisher SK. Neurons of the human retina: A golgi study. *Journal of Comparative Neurology*. 1992; 318:147–187. [PubMed: 1374766]
37. Pang JJ, Paul DL, Wu SM. Survey on amacrine cells coupling to retrograde-identified ganglion cells in the mouse retina. *Invest Ophthalmol Vis Sci*. 2013; 54:5151–5162. [PubMed: 23821205]
38. Kerrigan-Baumrind LA, Quigley HA, Pease ME, et al. Number of ganglion cells in glaucoma eyes compared with threshold visual field tests in the same persons. *Invest Ophthalmol Vis Sci*. 2000; 41:741–748. [PubMed: 10711689]
39. Rao HL, Leite MT, Weinreb RN, et al. Effect of disease severity and optic disc size on diagnostic accuracy of rtvue spectral domain optical coherence tomograph in glaucoma. *Invest Ophthalmol Vis Sci*. 2011; 52:1290–1296. [PubMed: 20811060]
40. Lisboa R, Paranhos A, Weinreb RN, et al. Comparison of different spectral domain OCT scanning protocols for diagnosing preperimetric glaucoma. *Invest Ophthalmol Vis Sci*. 2013; 54:3417–3425. [PubMed: 23532529]
41. Redmond T, Garway-Heath DF, Zlatkova MB, et al. Sensitivity loss in early glaucoma can be mapped to an enlargement of the area of complete spatial summation. *Invest Ophthalmol Vis Sci*. 2010; 51:6540–6548. [PubMed: 20671278]
42. Garway-Heath DF, Caprioli J, Fitzke FW, et al. Scaling the hill of vision: The physiological relationship between light sensitivity and ganglion cell numbers. *Invest Ophthalmol Vis Sci*. 2000; 41:1774–1782. [PubMed: 10845598]
43. Malik R, Swanson WH, Garway-Heath DF. 'Structure-function relationship' in glaucoma: Past thinking and current concepts. *Clin Experiment Ophthalmol*. 2012; 40:369–380. [PubMed: 22339936]
44. Tatham AJ, Weinreb RN, Zangwill LM, et al. The relationship between cup-to-disc ratio and estimated number of retinal ganglion cells. *Invest Ophthalmol Vis Sci*. 2013; 54:3205–3214. [PubMed: 23557744]

45. Chauhan BC, O'Leary N, Almobarak FA, et al. Enhanced detection of open-angle glaucoma with an anatomically accurate optical coherence tomography-derived neuroretinal rim parameter. *Ophthalmology*. 2013; 120:535–543. [PubMed: 23265804]

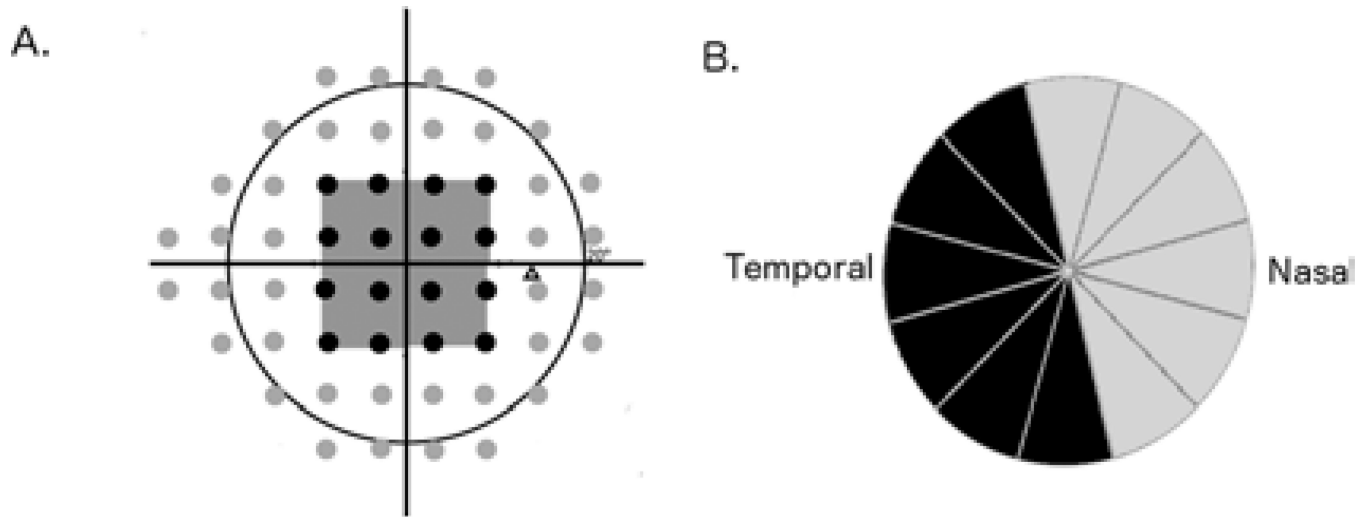


Figure 1.

Illustration of the 24-2 visual field map for the right eye showing test locations used for retinal ganglion cell estimates for total (black and grey points) and macular (16 black points corresponding to the central 10 degrees) estimates (A). Illustration of the 6 clock hours of the optical coherence tomography circumpapillary retinal nerve fiber layer thickness scan used for the structural component of the macular retinal ganglion cell number estimate (the black sectors in the figure) (B).

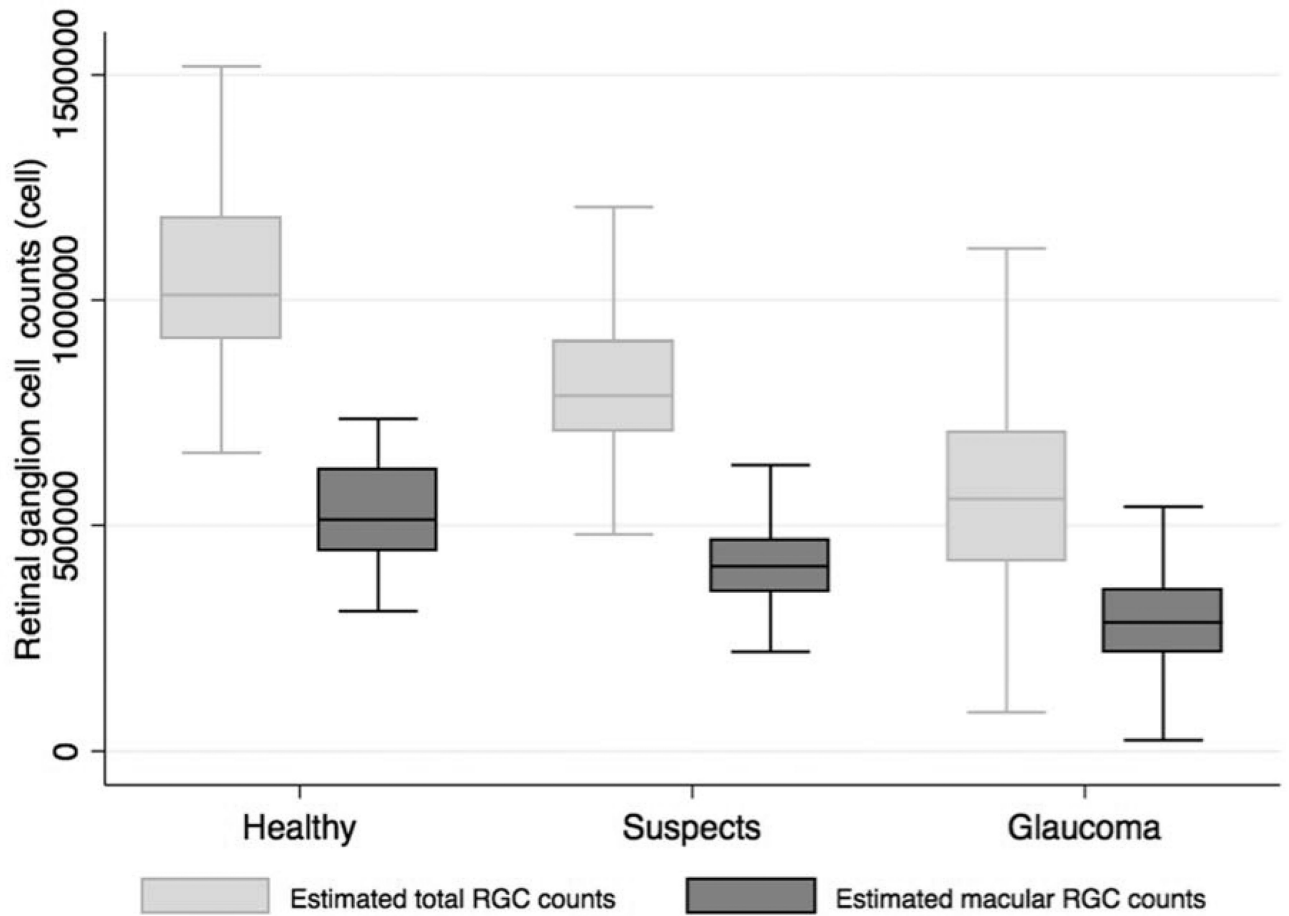


Figure 2. Boxplot illustrating the distribution of estimated number of macular retinal ganglion cells and total number of retinal ganglion cells in healthy, glaucoma suspects and glaucomatous eyes.

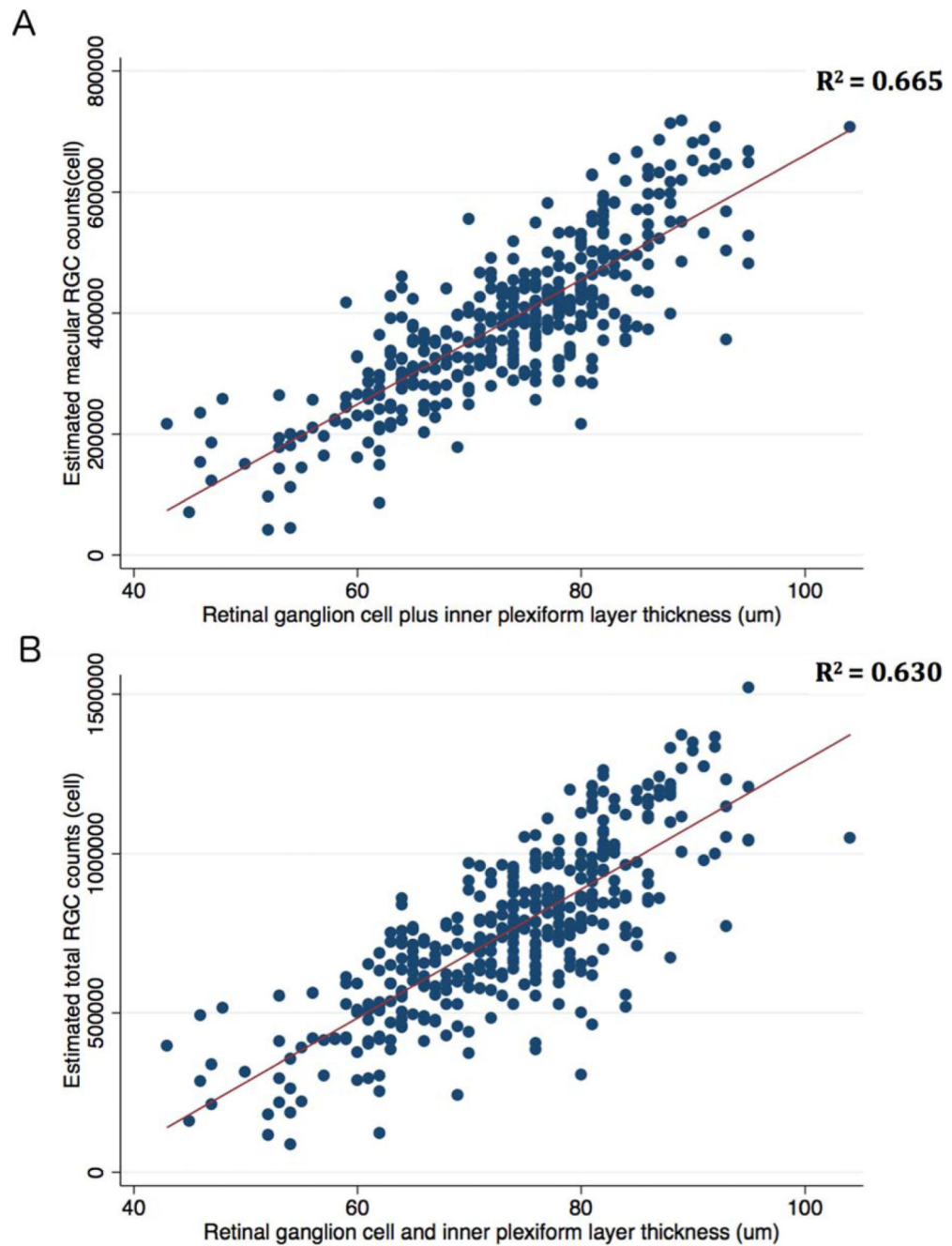


Figure 3. Scatterplots and ordinary least squares (OLS) regression lines showing the relationship between estimated number of macular RGCs and the macular ganglion cell inner plexiform layer (mGCIPL) thickness (A) and estimated total number of RGCs and mGCIPL thickness (B).

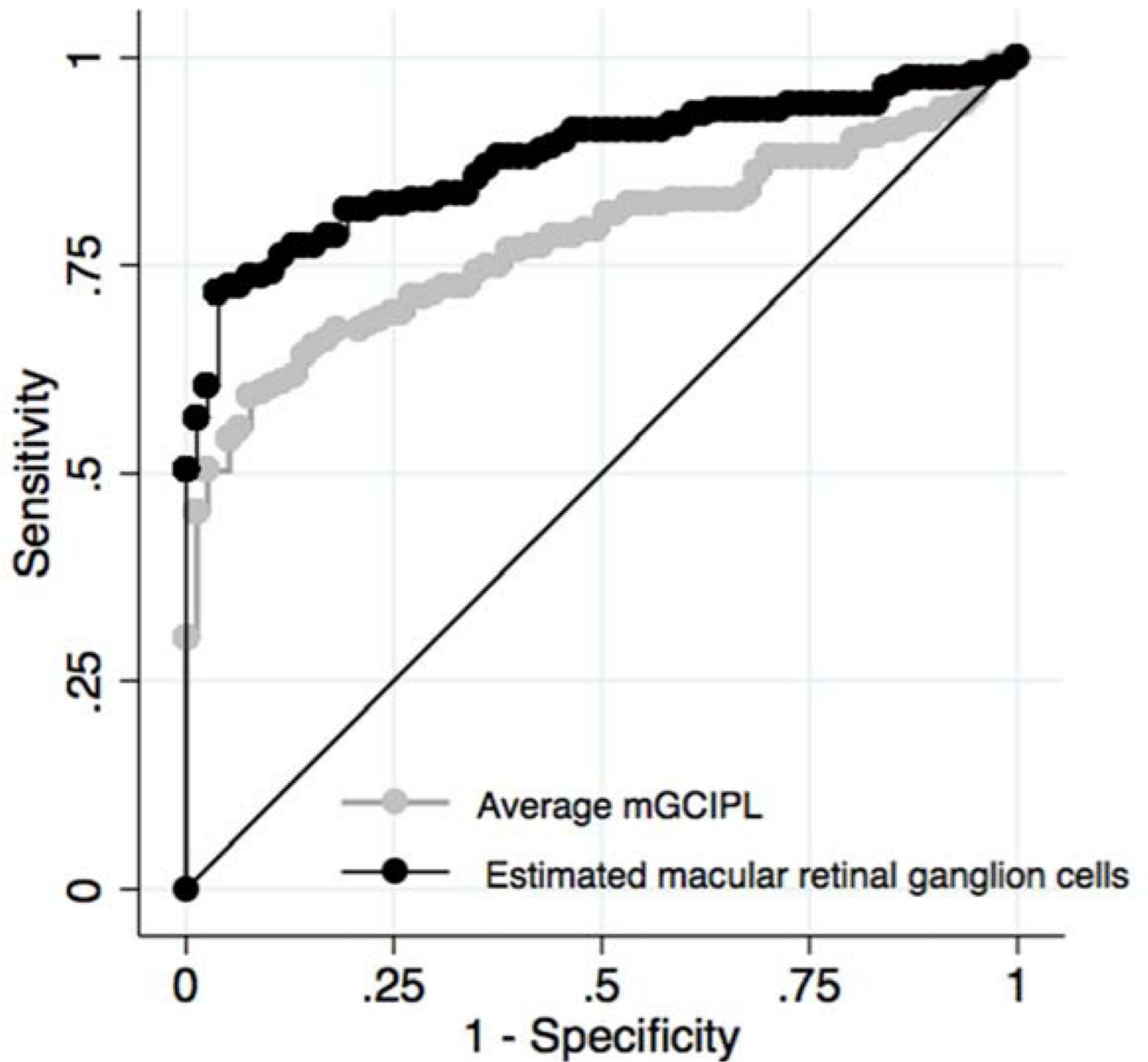


Figure 4. Receiver operating characteristic curves showing the ability of estimated number of macular retinal ganglion cells and the macular ganglion cell-inner plexiform layer (mGCIPL) thickness to differentiate glaucomatous and healthy eyes.

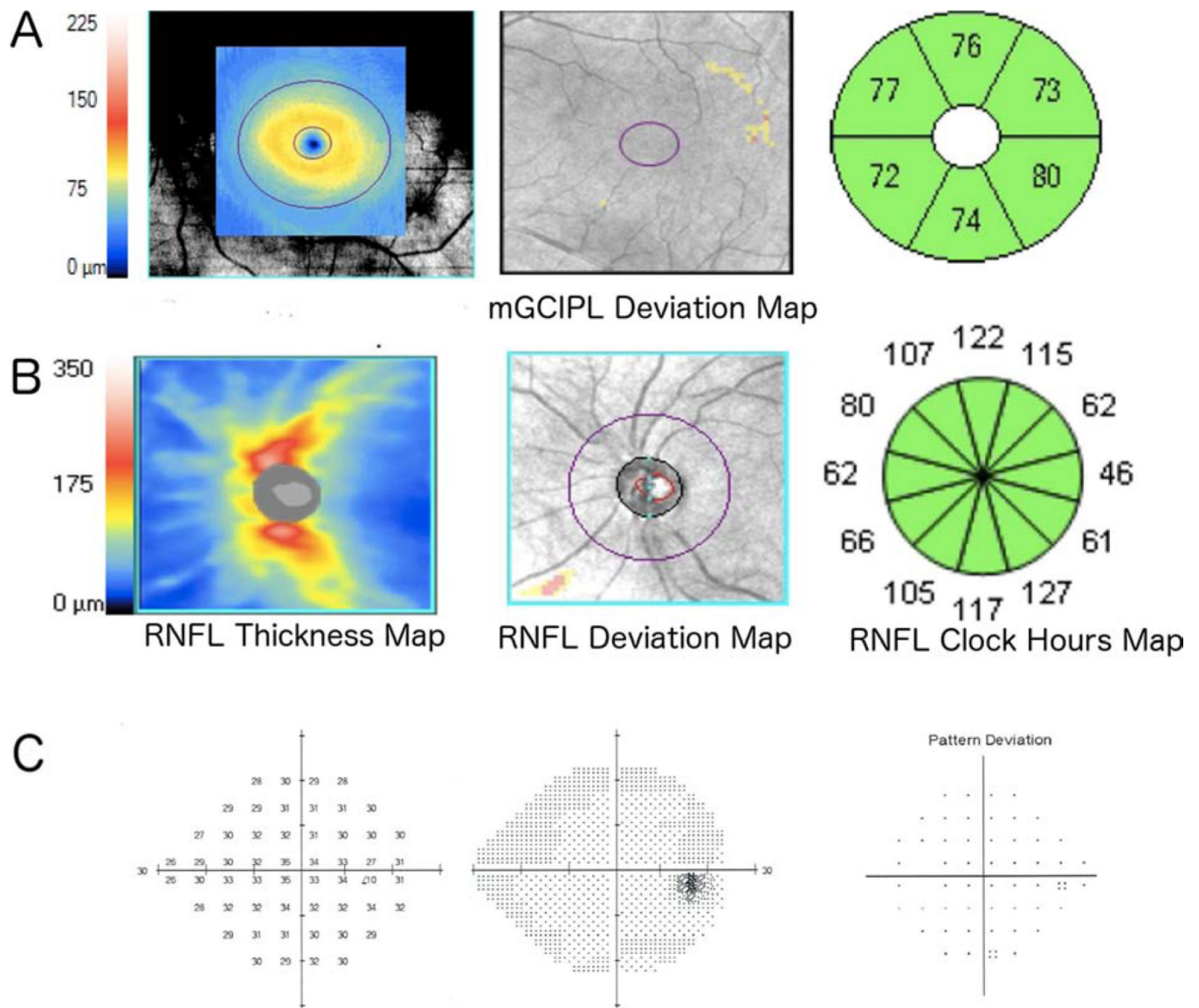


Figure 5. Example of a healthy left eye of a 66-year-old subject showing macular ganglion cell-inner plexiform layer (mGCIPL) thickness, deviation and thickness sectors maps (A), circumpapillary retinal nerve fiber layer (cpRNFL) thickness, deviation maps and RNFL thickness sector map (B), and standard automated perimetry (SAP) results (C). The average mGCIPL thickness was 76 μm and the estimated numbers of total and macular retinal ganglion cells (RGCs) were 941,711 and 448,087 cells, respectively.

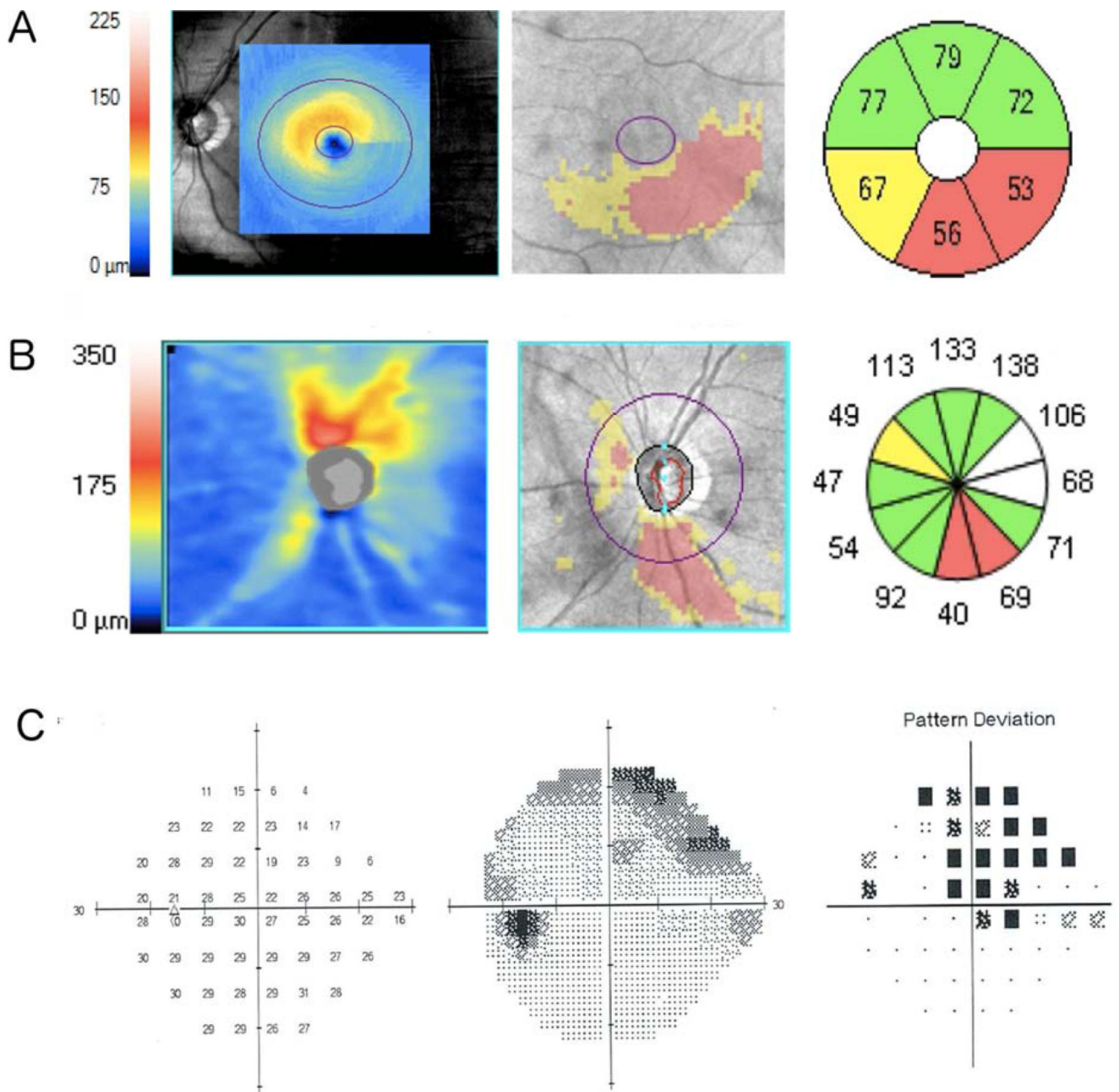


Figure 6. Example of a glaucomatous left eye of 64-year-old subject showing macular ganglion cell-inner plexiform layer (mGCIPL) thickness, deviation and thickness sectors maps (A), circumpapillary retinal nerve fiber layer (cpRNFL) thickness, deviation maps and thickness sectors maps (B), and standard automated perimetry (SAP) results (C). The mean mGCIPL thickness was 67 μm and the estimated numbers of total and macular retinal ganglion cells were 558,922 and 282,981 cells, respectively.

Table 1

Summary of Demographic and Clinical Characteristics of Healthy Eyes compared to those with Glaucoma and Suspected Glaucoma.

| | Healthy (n = 77 eyes, 42 subjects) | Glaucoma Suspects (n =154 eyes, 89 subjects) | Glaucoma (n =159 eyes, 93 subjects) |
|--|--|--|---|
| Age (years) | 49.16 ± 17.12 | 66.03 ± 12.48 | 70.87 ± 12.19 |
| Sex (number) | 25 (60 %) | 44 (49%) | 48 (52%) |
| Female | | | |
| Ancestry (number) | | | |
| European | 21(50%) | 67 (75%) | 57 (61%) |
| African | 16 (38%) | 19 (21%) | 28 (30%) |
| Other | 5(12%) | 3 (3%) | 8 (9%) |
| SAP VFI (%) | 99 ± 1 | 99 ± 3 | 87 ± 16 |
| SAP MD (dB) | 0.04 ± 1.02 | 0.47 ± 1.73 | -5.06 ± 5.43 |
| Macular SAP TD (dB) | -0.51 ± 0.56 | -0.86 ± 1.11 | -2.91 ± 3.24 |
| mGCIPL (μm) | 81.40 ± 6.71 | 75.545 ± 7.17 | 67.98± 10.73 |
| cpRNFL thickness (μm) | 93.04 ± 9.49 | 83.75 ± 10.71 | 73.13 ± 14.38 |
| Estimated macular RGC count (cells) | 520,678 ± 106,843 | 410,003± 83,887 | 306,010 ± 109,449 |
| Estimated total RGC count (cells) | 1,042,019 ± 185,243 | 812,458± 163,151 | 570,433 ± 207,525 |

Values correspond to mean ± standard deviation.

Abbreviations: VFI = visual field index; SAP = standard automated perimetry; MD = mean deviation; TD = total deviation; mGCIPL= macular ganglion cell layer plus inner plexiform layer; cpRNFL = circumpapillary retinal nerve fiber layer; RGC = retinal ganglion cell.